Lattice structures and electronic properties of CIGS/CdS interface: First-principles calculations*

Tang Fu-Ling(汤富领)[a)b)†], Liu Ran(刘 冉)[a)b)], Xue Hong-Tao(薛红涛)[a)], Lu Wen-Jiang(路文江)[a)], Feng Yu-Dong(冯煜东)[b)], Rui Zhi-Yuan(芮执元)[a)], and Huang Min(黄 敏)[c)]

[a)] *State Key Laboratory of Gansu Advanced Non-ferrous Metal Materials, Department of Materials Science and Engineering, Lanzhou University of Technology, Lanzhou* 730050, *China*

[b)] *Science and Technology on Surface Engineering Laboratory, Lanzhou Institute of Physics, Lanzhou* 730000, *China*

[c)] *State Key Laboratory of Magnetic Resonance and Atomic and Molecular Physics, Wuhan Institute of Physics and Mathematics, Chinese Academy of Sciences, Wuhan* 430071, *China*

(Received 2 December 2013; revised manuscript received 31 December 2013; published online 29 May 2014)

Using first-principles calculations within density functional theory, we study the atomic structures and electronic properties of the perfect and defective ($2V_{Cu}+In_{Cu}$) $CuInGaSe_2$/CdS interfaces theoretically, especially the interface states. We find that the local lattice structure of ($2V_{Cu}+In_{Cu}$) interface is somewhat disorganized. By analyzing the local density of states projected on several atomic layers of the two interfaces models, we find that for the ($2V_{Cu}+In_{Cu}$) interface the interface states near the Fermi level in $CuInGaSe_2$ and CdS band gap regions are mainly composed of interfacial Se-4p, Cu-3d and S-3p orbitals, while for the perfect interface there are no clear interface states in the $CuInGaSe_2$ region but only some interface states which are mainly composed of S-3p orbitals in the valance band of CdS region.

Keywords: first-principles calculation, $CuInGaSe_2$/CdS, density of states, interface states

PACS: 73.20.−r, 02.60.Cb, 73.20.At **DOI:** 10.1088/1674-1056/23/7/077301

1. Introduction

Thin film ZnO/CdS/chalcopyrite solar cells have received much attention due to their superior overall performances of low cost, radiation hardness, long term stability, and high efficiency.[1] Cu(In,Ga)Se_2 (CIGS) chalcopyrite alloys provide absorber materials for the most efficient solar cells of this kind. Their photoelectric conversion efficiencies have reached above 20% in the laboratory.[2] The existences of surfaces and interfaces destroy the three-dimensional symmetry of the crystal, resulting in additional states at surfaces and interfaces, thereby making the performance of heterojunction different from that of the bulk. In recent years, studies on the properties of the surface and interface have received much attention.[3–8]

To a large extent, the electronic performance of the CIGS thin film solar cell depends on the interface structure and electronic properties between CIGS and the buffer layer CdS, in which the internal electric field is formed. Hence it affects the charge transport through the PN junction. CIGS/CdS interface may introduce extra electronic states into the band gap as a result of lattice mismatch or the existence of interface defects. These extra states prevent the photo-generated carriers from passing through the Fermi level, resulting in a reduction of the band gap, thereby reducing the open-circuit voltage. In order to improve the properties of CIGS solar cells, it is important to understand the local lattice structure near the CIGS/CdS interface and the origins of the interface states.

From experiments, some studies on the CIGS/CdS interface relied on spectroscopic methods. Using energy dispersive X-ray spectroscopy, Auger electron spectroscopy, and secondary ion mass spectrometry techniques, the absorber/buffer interface was found to be intermixed.[9–11] Some researchers have found that a Cu-depleted and Cd-doped region is incorporated into the first several atomic layers of the $CuInSe_2$.

On the theoretical research side, there are few studies directly dealing with the CIGS/CdS interface states, but some theoretical studies were performed on the details of band structures and alignments,[12–14] especially the valence band offsets and conduction band offsets. Favorable band offsets may be fine for a high open-circuit voltage. Hinuma *et al.*[14] also calculated the density of states for each layer of the $CuInSe_2$/CdS (110) interfaces using first-principles calculations. They found that in the ($Cu_{In}+In_{Cu}$) interface some interface states are located at the top of the valance band of CIS and in the CdS region.

Although plenty of experimental and some calculated results are given to understand the chemical composition and band alignments of CI(G)S/CdS interfaces, the lattice structures, band structures and the interface states of CIGS/CdS interface have been little investigated on an atom-scale. In this paper, we use the first-principles calculation[15,16] to study the local lattice structures and electronic properties of CIGS/CdS interface, especially in the interface states. We also compare

*Project supported by the National Natural Science Foundation of China (Grant Nos. 11364025 and 11164014) and the Gansu Science and Technology Pillar Program, China (Grant No. 1204GKCA057).

†Corresponding author. E-mail: tfl03@mails.tsinghua.edu.cn

© 2014 Chinese Physical Society and IOP Publishing Ltd

our results with previous experimental and calculated results.

2. Computational methods

The projector augmented wave (PAW) method as implemented in the Vienna *ab initio* simulation package (VASP)[17] is used. The generalized gradient approximation (GGA) functional of Perdew–Burke–Ernzerhof (PBE) is adopted to describe the exchange–correlation energy. In this pseudopotential approach, core electrons that do not participate in the bonding characteristic of the material are frozen and only valence electrons are taken into account. For the pseudopotentials used here, the electronic configurations are [Ar] $3d^{10}4s^1$, [Kr] $5s^25p^1$, [Ar] $4s^24p^1$, [Ar] $4s^24p^4$, [Kr] $4d^{10}5s^2$, and [Ne] $3s^23p^4$ for copper, indium, gallium, selenium, cadmium, and sulfur, respectively. Here, Γ-centered k-point meshes of $6\times6\times3$, $5\times5\times5$, $2\times1\times1$, and $2\times1\times1$ are used for calculating the bulk $CuInSe_2$, bulk CdS, CIS (112) surface, and CIGS/CdS interfaces, respectively. The plane wave energy cutoff of 450 eV and the conjugate gradient (CG) method are applied to the atomic structure optimization.

The most widely used method in electronic structure simulation,[18] density functional theory (DFT), as is well known, underestimates semiconductor band gaps. A better solution for this question is to use the HSE06 functional, a hybrid functional with a partial Hartree–Fock screening proposed by Heyd *et al.*[19] for DFT calculation. We have used HSE06 functional to predict the optical properties of Al-[20] and S-doped[21] $CuInSe_2$. However HSE06 is too time-consuming, especially for the calculation on the interface structure. Some studies suggest that GGA+U method is more appropriate to calculate the electronic properties of materials.[22,23] Thus, in this paper, the band gap problem on $Cu(In,Ga)Se_2$ is addressed by adding a Hubbard U correction to the GGA energy functional acting on the 3d states of Cu atoms. We select a value of the parameter U to be 8 eV, in view of the results of other studies with U-value correction calculations[14,24–27] and computational time.

3. Results and discussion

3.1. Electronic properties of bulk $CuInSe_2$ and CdS

$CuInSe_2$ (CIS) belongs to the group of I–III–VI_2 semiconductor materials and crystallizes into a tetragonal chalcopyrite structure (space group $I42d$ as shown in Ref. [28]). CdS is one of the group II–VI compound semiconductors and exists mainly in sphalerite structure in nature (space group $F43m$ also as shown in Ref. [28]), which can be used as a suitable buffer layer for CIS based photovoltaic (PV) device.[29] The calculated structure parameters a, c and bond lengths d_{Cu-Se} and d_{In-Se} of CIS are displayed in Table1 and compared with other calculated[30] data and also with experimental data determined by X-ray powder[31,32] or single crystal diffraction.[33] The calculated lattice parameter a of CdS is 5.925 Å (experimental value of a is 5.818 Å[34]). It can be seen that the calculated lattice parameters of bulk CIS and CdS are slightly larger than the experimental values.

Table 1. Calculated values of lattice parameters a, c, and bond lengths d_{Cu-Se} and d_{In-Se} of $CuInSe_2$ bulk. and their comparison with room temperature experimental data.

a/Å	c/Å	d_{Cu-Se}/Å	d_{In-Se}/Å	Method
5.869	11.823	2.460	2.641	*ab initio*[a]
5.880	11.833	2.447	2.665	*ab initio*[b]
5.782(1)	11.620(1)	2.458	2.559	X-ray power diffr.[c]
5.784(1)	11.616(5)	2.424	2.598	X-ray power diffr.[d]
5.781(1)	11.642(3)	2.433	2.589	X-ray single cryst. diffr.[e]

[a] This work, [b] Ref. [30], [c] Ref. [31], [d] Ref. [32], [e] Ref. [33].

The calculated band structure and density of states (DOS) of bulk CIS are shown in Fig. 1, in which the Fermi level is set at 0 eV. From Fig. 1(a), we can see that the calculated band gap is 0.4 eV by GGA+U, while the gap value is 0.014 eV by GGA. Hinuma *et al.*[14] obtained the band gap to be 0.08 eV by GGA+U($U-J=5$ eV), and Jiang and Feng[35] obtained the band gap to be 0.2 eV by GGA. The calculated band gaps are lower than the experimental value (1.04 eV). As seen in Fig. 1(a), the top of the valence band and the bottom of the conduction band lie along the gamma-point, indicating that this compound is a direct band gap semiconductor. As seen in Fig. 1(b), the uppermost valence band is derived from a combination of the p orbital of Se atoms and the d orbital of the Cu atoms, while the bottom of the conduction band is mainly derived from the s orbital of In atoms. Our calculated results are consistent with the results in Ref. [36].

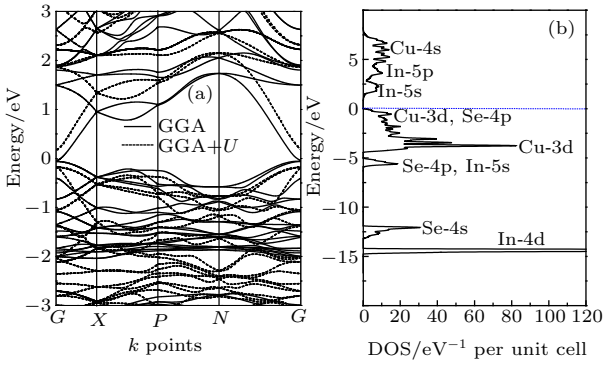


Fig. 1. (a) Band structures of bulk $CuInSe_2$ using GGA (solid line) and GGA+U (dashed line) ($U=8$ eV); (b) DOS of bulk $CuInSe_2$ calculated by GGA+U ($U=8$ eV). Fermi level is set at zero energy in the paper unless otherwise stated.

In addition, we calculate the band structure and DOS of bulk CdS (shown in Fig. 2). The calculated direct band gap of CdS is 1.12 eV, larger than a theoretical value 0.806 eV,[37] and smaller than a theoretical result 2.39 eV,[38] and experimental value 2.42 eV.[39] As seen in Fig. 2(b), the uppermost valence band is derived from S-3p orbital, while the bottom of

conduction band is derived from Cd-5s orbital. This finding is in agreement with the result in Ref. [37].

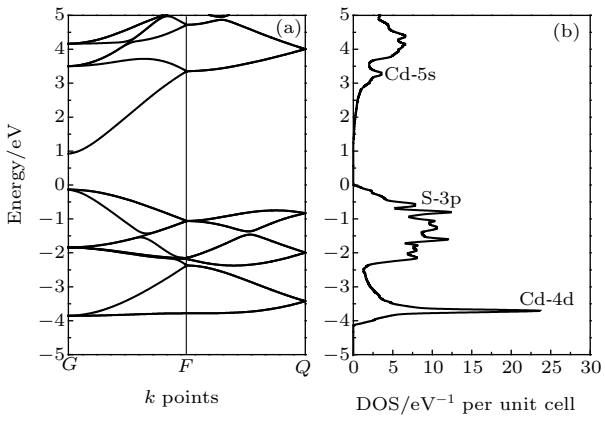


Fig. 2. Band structure (a) and density of states (b) of bulk CdS.

3.2. Electronic properties of CIS (112) surface

Besides bulk CIS and bulk CdS, CIS (112) surface and CIGS/CdS interfaces are constructed. The (112) surface is always considered to be the natural growth surface of $CuInSe_2$[40–44] and hence predominant in the grains in high-quality polycrystalline solar cell absorber film. Rockett[44] found that the {112} planes are the lowest energy surfaces with the cation-terminated surface having a lower overall energy than the anion-terminated surface. Hence, we use a cation-terminated surface model including 112 atoms, in which periodic boundary conditions are applied to the surface supercell including seven CIS bilayers and a vacuum region ($\sim$ 20 Å) as shown in Fig. 3(a). The lattice parameters $a = 8.3013$ Å and $b = 14.466$ Å. During the calculations, four atomic layers are fixed. Because CIS (112) surface is a polar face, a dipole correction is made along the thickness direction in the surface and interface calculations.

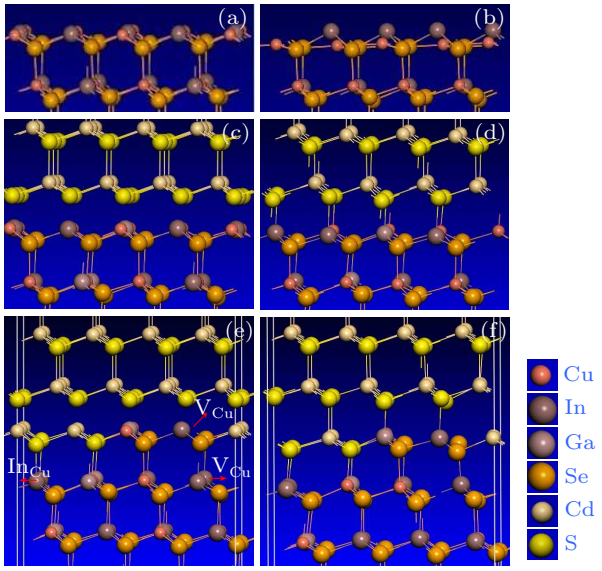


Fig. 3. (color online) Lattice structures of the CIS (112) surface ((a), (b)), the perfect CIGS/CdS interface ((c), (d)), and the ($2V_{Cu}+In_{Cu}$) CIGS/CdS interface ((e), (f)). Panels (a), (c), and (e) show the original structures, while panels (b), (d), and (f) display the relaxed structures.

The calculated (112) surface after relaxation is shown in Fig. 3(b). On the outmost layer, Cu atoms move inwards by 0.014 Å, while In atoms move outwards by 0.006 Å. The values of bond length $d_{Cu–Se}$ are 2.339–2.372 Å, and the values of $d_{In–Se}$ are 2.696–2.743 Å, while in $CuInSe_2$ bulk the $d_{Cu–Se}$ is 2.460 Å, and $d_{In–Se}$ is 2.641 Å: $d_{Cu–Se}$ contracts by about 4% and $d_{In–Se}$ expands by about 3%. On the second layer, the values of bond length $d_{Cu–Se}$ are 2.449–2.466 Å and $d_{In–Se}$ are 2.657 Å, similar to the bulk values. Figure 4 shows part of the band structure and DOS of the ideal CIS (112) surface, revealing some surface states (dashed lines) within the gap region of bulk material. These states are in the vicinity of the Fermi level. Hinuma *et al.*[45] also obtained the particular states in the faceted (112) surfaces (with defects $Cu_{In}+In_{Cu}$ mostly localized on the second layer), which are distributed up to approximately 0.2 eV above the bulk VBM (set at zero energy) and attributed to Cu and Se components (see Fig. 6 in Ref. [45]). In contrast, Rodriguez *et al.*[40,41] found the surface states close to the bottom of the conduction band of the ideal bulk crystal. This difference may be caused by different calculation methods and the differences in used model structure between different methods. We use pseudopotential density functional theory (DFT) with the generalized gradient corrected Perdew–Burke–Ernzerhof (PBE) for the exchange and correlation functional, whereas Rodriguez et al. used the surface Green's function matching (SGFM) method, a method of Cunningham integration in the first Brillouin zone.

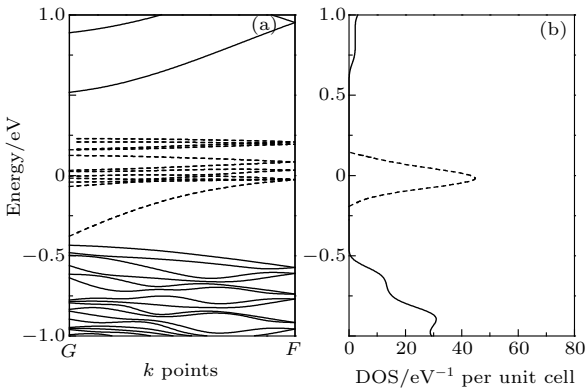


Fig. 4. (a) Band structure and (b) DOS of CIS (112) surface, where dashed lines show the surface states.

We also calculate the DOS (Fig. 5) projected onto the outmost layer and that on the fourth layer below the surface. The fourth layer from the surface can be considered as the bulk atoms, because its electronic properties are affected slightly by the surface. From Fig. 5, we can see that surface states, the additional energy states due to the presence of the surface, are mainly formed by Se-4p orbital and In-5s orbital electrons. This is because the lattice is terminated abruptly at the surface, per atom on the outermost layer of the surface will have unpaired electrons, that is, an unsaturated bond (the so-called dangling bond).

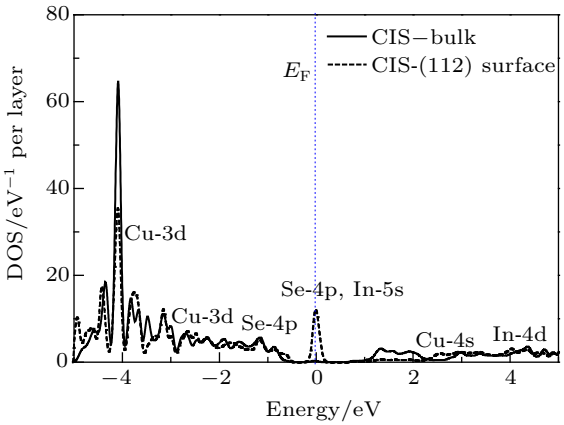


Fig. 5. DOSs projected onto several atomic layers of CIS (112) surface, where dashed line represents the DOS of surface atoms; the solid line denotes the DOS of the atoms on the fourth layer below the surface (considered as bulk atoms).

3.3. Electronic properties of CIGS/CdS interface

The band gap of CIS is relatively low (1.04 eV), slightly below the range of high conversion efficiency of solar cell. In order to increase the band gap to a desired value and to achieve enhanced current conversion efficiency, Ga substitution for In (Cu(In,Ga)Se_2) is probably the best option.[46–48] The high-efficiency devices are based on absorbers with a Ga/(In + Ga) ratio of approximately 0.25–0.33, corresponding to a band gap energy (E_g) of approximately 1.1–1.2 eV.[49] Hence, we study the lattice structure and electronic properties of $CuIn_{0.75}Ga_{0.25}Se_2$ (CIGS)/CdS interface.

The perfect interface is composed of two parts: the lower part contains seven bilayers of cation-terminated $CuIn_{0.75}Ga_{0.25}Se_2$(112) planes, and the upper part contains six bilayers of CdS ($1\times1\times2$) superlattice (112) planes. Although CdS (111) surface is a close-packed surface and has the lowest surface energy, it has a poor lattice mismatch with CIGS (112) surface. However, the lattice structure of CdS ($1\times1\times2$) supercell is consistent with that of CIGS material, and the CdS ($1\times1\times2$) superlattice (112) plane is the same as CdS (111) plane essentially and has a better lattice mismatch (less than 1.0%) with CIGS (112) plane. The model includes 206 atoms, and the lattice parameters $a = 8.313$ Å, $b = 14.28$ Å. A 20-Å vacuum region is used to avoid the interactions between the surface atoms and the atoms in the periodic slabs. The bottom and top atoms are passivated by pseudohydrogen to ensure that there are no dangling bonds at the top (CdS) and bottom (CIGS) surfaces. We perform a relaxation, with the bottom three layers of CIGS and the top three layers of CdS layers fixed in the calculation process. The perfect lattice structure is shown in Fig. 3(c), and the lattice structure after relaxation is shown in Fig. 3(d). We can see that the positions and the bond lengths of atoms on the interface change slightly: after relaxation the bond lengths of $d_{Cu–Se}$, $d_{Ga–Se}$, $d_{In–Se}$, and $d_{Cd–S}$ are 2.449 Å, 2.457 Å, 2.630 Å, and 2.571 Å respectively, while before relaxation the bond lengths of $d_{Cu–Se}$, $d_{Ga–Se}$, $d_{In–Se}$, and $d_{Cd–S}$ are 2.454 Å, 2.496 Å, 2.655 Å, and 2.542 Å.

As described in the Introduction, the actual CIGS/CdS interface is not perfect, so in the modeling process we artificially added some defects.[50,51] to simulate the actual interface, which was named ($2V_{Cu}+In_{Cu}$) interface as shown in Fig. 3(e). Specifically, on the CIGS layer connected with CdS layers, half of Cu, In atoms are replayed by Cd atoms and half of Se atoms are replayed by S atoms for mimicking the atomic diffusion in the interface and half of remaining Cu atoms become Cu vacancies (V_{Cu}). We name this layer the interface layer, on which the chemical composition is $CuInGaSe_4+Cd_4S_4$. On the first layer below the interface layer (in the CIGS region), a Cu atom becomes V_{Cu} and a Cu atom is changed into In atom (In_{Cu}), the chemical composition was $Cu_2In_4GaSe_4$.

The presences of Cd–Se, Cd–S, Cu/Ga–S, In–Se bonding at CIGS/CdS interfaces introduce more complicated atomic structures than at perfect CIGS/CdS interfaces (Fig. 3(c)). We can see that the ($2V_{Cu}+In_{Cu}$) interface becomes somewhat disorganized after relaxation from Fig. 3(f): on the interface layer, the values of bond lengths $d_{Cu–Se}$,$d_{Ga–Se}$, $d_{In–Se}$, $d_{Cd–Se}$, $d_{Cd–S}$, $d_{Cu–S}$, and $d_{Ga–S}$ are 2.45 Å, 2.397–2.45 Å, 2.522 Å, 2.514 Å, 2.532Å, 2.310Å, and 2.353 Å respectively. On the first layer below the interface layer, the values of bond lengths $d_{Cu–Se}$, $d_{Ga–Se}$, and $d_{In–Se}$ are 2.413–2.477 Å, 2.428 Å, and 2.618–2.683 Å respectively, and on the first layer above the interface layer, $d_{Cd–S}$ is in a range of 2.483–2.632 Å. Before relaxation, the values of bond lengths $d_{Cu–Se}$, $d_{Ga–Se}$, $d_{In–Se}$, $d_{Cd–Se}$, $d_{Cd–S}$, $d_{Cu–S}$, and $d_{Ga–S}$ are 2.454 Å , 2.494 Å, 2.649 Å, 2.666 Å, 2.651 Å, 2.469 Å, and 2.509 Å, respectively.

We study the DOSs of the perfect and ($2V_{Cu}+In_{Cu}$) interfaces. Our calculation shows that the fourth CdS layer away from the interface has the electronic structure the same as that of CdS bulk, so does the fourth $CuInGaSe_2$ layer. As can be seen from Fig. 6, there are extra electronic states lying close to the CIGS valence band (VB) edges of the two interface models. For the perfect interface, there is only one clear extra state peak at the Fermi level. For the ($2V_{Cu}+In_{Cu}$) interface, apart from the state peak at the position about −0.1 to 0.3 away from the Fermi level, there still is another extra state peak at −0.4 to −0.1 eV away from the Fermi level. We can also see that the density peak in the vicinity of the Fermi level at the ($2V_{Cu}+In_{Cu}$) interface is higher than at the perfect interface, suggesting that the defects and atomic diffusion at the ($2V_{Cu}+In_{Cu}$) interface increase the interface recombination effects.

However, through calculating the DOSs of the several layers atoms in the two interface models (see Fig. 7), we find that there are no clear additional states at the position between

about −0.1 to 0.3 eV away from the Fermi level in the two interface models. Therefore, we suspect that the peaks appearing in the vicinity of the Fermi level (in Fig. 6) are mixture results of interface states and the surface states. The peak at the position about −0.4 to −0.1 away from the Fermi level comes from the interfacial electron distribution; and the peak at the position about −0.1 to 0.3 away from the Fermi level comes from the surface atomic electron distribution. Although we have passivated the two surfaces by pseudohydrogen in calculation, the surface states may still exist to some extent, and this hypothesis has been confirmed by calculating the DOSs of atoms on the uppermost and lowermost layers (not shown).

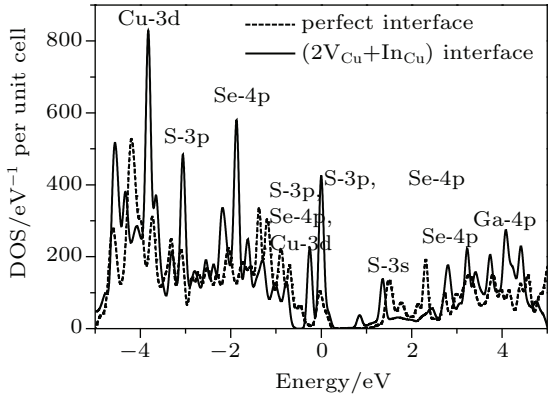


Fig. 6. DOSs of perfect and the (2V$_{Cu}$+In$_{Cu}$) interfaces, where dashed line represents DOS of the perfect interface, the solid line represents DOS of the the (2V$_{Cu}$+In$_{Cu}$) interface.

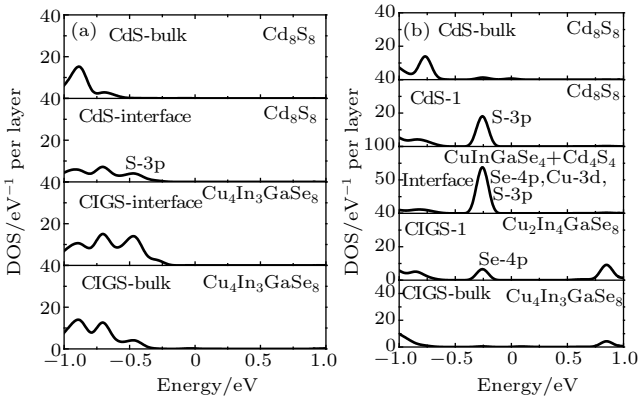


Fig. 7. DOSs projected onto different CuInGaSe$_2$ and CdS layers on (a) the perfect interface depicted in Fig. 3(c) and (b) the (2V$_{Cu}$+In$_{Cu}$) interface depicted in Fig. 3(e).

From Fig. 7, we can see that for the perfect interface there are no clear interface states in the CIGS region, and there are additional states composed mainly of S-3p orbital in the CdS region (marked by "S-3p"). In the (2V$_{Cu}$+In$_{Cu}$) interface, there are some extra electronic states induced by Se-4p, Cu-3d and S-3p in the gap region of CIGS and CdS sides between about −0.4 to −0.1 eV below the Fermi level in the interface supercell (marked by "Se-4p", "Cu-3d" and "S-3p"). These states may prevent the photo-generated carriers from passing through the Fermi level, thereby reducing the open-circuit voltage. These results are in agreement with those of CuInSe$_2$(CIS)/CdS (110) interface.[14] In faceted and nonfaceted CIS/CdS (110) interfaces, there are no clear interface states in the CIS region, while there are interface states composed mainly of S-3p orbitals in the CdS region. In the (Cu$_{In}$+In$_{Cu}$) interface, there are some interface states at the top of the valance band of CIS formed by Cu-3d and Se-4p orbitals, and there are also interface states in the CdS region, which are composed of S-3p orbitals.[14]

The origins of the interface states can be explained in terms of local charge transfer. A Bader charge analysis (see Table 2) on the (2V$_{Cu}$+In$_{Cu}$) interface shows that the electric charges of the interfacial Cu (Cu$^{0.36+}$), In (In$^{1.05+}$) and Ga (Ga$^{1.06+}$) are more than those of bulk Cu (Cu$^{0.27+}$), In (In$^{1.02+}$) and Ga (Ga$^{0.94+}$), respectively. The electric charges of the interfacial Se (Se$^{0.6-}$) and S (S$^{0.8-}$) are less than those of bulk Se (Se$^{0.65-}$) and S (S$^{0.87-}$), respectively. These small electric charge losses of the interfacial atoms are mainly responsible for introducing the gap states.

Table 2. Atomic charges of bulk and interfacial atoms for the perfect interface and (2V$_{Cu}$+In$_{Cu}$) interface.

	Bulk S	Bulk Cd	Bulk Cu	Bulk In	Bulk Ga	Bulk Se
Perfect	6.87	11.14	10.73	11.98	12.06	6.65
2V$_{Cu}$+In$_{Cu}$	6.87	11.14	10.73	11.98	12.06	6.65
	Inter. S	Inter. Cd	Inter. Cu	Inter. In	Inter. Ga	Inter. Se
Perfect	6.84	11.13	10.67	11.91	12.01	6.64
2V$_{Cu}$+In$_{Cu}$	6.80	11.12	10.64	11.95	11.94	6.60

The interface states are generated possibly by defects or by surface contaminants.[52] The surface of calculated interface model is clean, hence defects mechanism can be used to explain our research results. We suspect that the chemical compositions of the interfacial atoms are non-stoichiometric, that is, unsaturated bonds are generated at the interface, resulting in interface states in the band gap.

4. Conclusions

In this paper, we study the local lattice structures and electronic properties of bulk CuInSe$_2$ (CIS), bulk CdS, CuInSe$_2$ (112) surface, and CuIn$_{0.75}$Ga$_{0.25}$Se$_2$ (CIGS)/CdS interfaces by using the first-principles calculations. The main findings are as follows. i) There are several additional states which are comprised of Se-4p and In-5s orbital near the Fermi level on the CIS surface. ii) The defective (2V$_{Cu}$+In$_{Cu}$) interface model becomes more disorganized after relaxation than the perfect interface. iii) For the perfect interface there are no clear interface states in the CIGS region and only some interface states are mainly composed of S-3p orbital in the CdS region. iv) For the (2V$_{Cu}$+In$_{Cu}$) interface there are some extra electronic states in the CIGS and CdS band gap regions between about −0.4 and −0.1 eV away from the Fermi level

in the interface supercell, resulting in a reduction of the band gap. These states mainly consist of interfacial Se-4p, Cu-3d, and S-3p.

Acknowledgment

This work was done at the Gansu Supercomputer Center.

References

[1] Turcu M and Rau U 2003 *J. Phys. Chem. Solids* **64** 1591
[2] Jackson P, Hariskos D, Lotter E, Paetel S, Wuerz R, Menner R, Wischmann W and Powalla M 2011 *Prog. Photovoltaics Res. Appl.* **19** 894
[3] Shi S Q, Tanaka S and Kohyama M 2006 *Model. Simul. Mater. Sc.* **14** S21
[4] Shi S Q, Tanaka S and Kohyama M 2007 *Phys. Rev. B* **76** 075431
[5] Wang W C, Xiong K, Lee G, Min H, Wallace R M and Cho K 2010 *Appl. Surf. Sci.* **256** 6569
[6] Lu H, Shen D H, Xue Q K, Polak M and Froumin N 2001 *Chin. Phys. Lett.* **18** 94
[7] Lei H, Liu C H, Lin B X and Fu Z X 2005 *Chin. Phys. Lett.* **22** 185
[8] Li M, Zhang J Y, Zhang Y and Wang T M 2012 *Chin. Phys. B* **21** 067302
[9] Cojocaru-Miredin O, Choi P, Wuerz R and Raabe D 2011 *Appl. Phys. Lett.* **98** 103504
[10] Cojocaru-Mirédin O, Choi P, Wuerz R and Raabe D 2012 *Appl. Phys. Lett.* **101** 181605
[11] Liao D and Rockett A 2003 *J. Appl. Phys.* **93** 9380
[12] Bao W and Ichimura M 2012 *Int. J. Photoenergy* **2012** 619812
[13] Minemoto T, Matsui T, Takakura H, Hamakawa Y, Negami T, Hashimoto Y, Uenoyama T and Kitagawa M 2001 *Sol. Energ. Mater. Sol. C* **67** 83
[14] Hinuma Y, Oba F, Kumagai Y and Tanaka I 2013 *Phys. Rev. B* **88** 035305
[15] Tang Y H, Zhang H, Cui L X, Ouyang C Y, Shi S Q, Tang W H, Li H, Lee J-S and Chen L Q 2010 *Phys. Rev. B* **82** 125104
[16] Shi S Q, Tanaka S and Kohyama M 2006 *Mater. Trans.* **47** 2696
[17] Kresse G and Furthmüller J 1996 *Phys. Rev. B* **54** 11169
[18] Shi S Q, Tanaka S and Kohyama M 2007 *J. Am. Ceram. Soc* **90** 2429
[19] Heyd J, Scuseria G and Ernzerhof M 2003 *J. Chem. Phys.* **118** 8207
[20] Wan F C, Tang F L, Zhu Z X, Xue H T, Lua W J, Feng Y D and Rui Z Y 2013 *Mater. Sci. Semicon. Process.* **16** 1422
[21] Zhu Z X, Tang F L, Lu W J, Feng Y D, Wang Z M and Wang Y 2012 *Physica B* **407** 4814
[22] Wang W H, Zhao G Z and Liang X X 2013 *Chin. Phys. B* **22** 120205
[23] Wu H P, Deng K M, Tan W S, Xiao C Y, Hu F L and Li Q X 2009 *Chin. Phys. B* **18** 5008
[24] Liechtenstein A, Anisimov V and Zaanen J 1995 *Phys. Rev. B* **52** R5467
[25] Lany S and Zunger A 2005 *Phys. Rev. B* **72** 035215
[26] Vidal J, Botti S, Olsson P, Guillemoles J F and Reining L 2010 *Phys. Rev. Lett.* **104** 056401
[27] Szabová L, Camellone M F, Huang M, Matolín V and Fabris S 2010 *J. Chem. Phys.* **133** 234705
[28] Müller J, Nowoczin J and Schmitt H 2006 *Thin Solid Films* **496** 364
[29] Chen D S, Yang J, Xu F, Zhou P H, Du H W, Shi J W, Yu Z S, Zhang Y H, Bartholomeus B and Ma Z Q 2013 *Chin. Phys. B* **22** 018801
[30] Lazewski J, Neumann H, Parlinski K, Lippold G and Stanbery B 2003 *Phys. Rev. B* **68** 144108
[31] Parkes J, Tomlinson R and Hampshire M 1973 *J. Appl. Crystallogr.* **6** 414
[32] Spiess H W, Haeberlen U, Brandt G, Räuber A and Schneider J 1974 *Phys. Status Solidi B* **62** 183
[33] Knight K 1992 *Mater. Res. Bull.* **27** 161
[34] Lin Y M, Ji Z H and Zeng X H 2008 *Journal of Yangzhou University* **11** 32 (in Chinese)
[35] Jiang F and Feng J 2006 *Appl. Phys. Lett.* **89** 221920
[36] Belhadj M, Tadjer A, Abbar B, Bousahla Z, Bouhafs B and Aourag H 2004 *Phys. Status Solidi B* **241** 2516
[37] Ni L H, Liu Y and Song C L 2008 *Rare Metal Mater. Eng.* **37** 623 (in Chinese)
[38] Ekuma E C, Bagayoko D, Zhao G L, Franklin L and Wang J T 2010 *AJP* **3** 119
[39] Pardo-Yissar V, Katz E, Wasserman J and Willner I 2003 *J. Am. Chem. Soc.* **125** 622
[40] Rodríguez J A, Quiroga L, Camacho A and Baquero R 1996 *Braz. J. Phys.* **26** 274
[41] Rodríguez J A, Quiroga L, Camacho A and Baquero R 1999 *Phys. Rev. B* **59** 1555
[42] Siebentritt S, Papathanasiou N, Albert J and Lux-Steiner M C 2006 *Appl. Phys. Lett.* **88** 151919
[43] Zhou Z, Zhao K, Wang Y M and Huang F Q 2011 *J. Inorg. Mater.* **26** 113
[44] Rockett A 2012 *Prog. Photovoltaics Res. Appl.* **20** 575
[45] Hinuma Y, Oba F, Kumagai Y and Tanaka I 2012 *Phys. Rev. B* **86** 245433
[46] Gloeckler M and Sites J 2005 *J. Phys. Chem. Solids* **66** 1891
[47] Birkmire R W 2001 *Sol. Energ. Mater. Sol. C* **65** 17
[48] Shafarman W N, Klenk R and McCandless B E 1996 *J. Appl. Phys.* **79** 7324
[49] Repins I, Contreras M A, Egaas B, DeHart C, Scharf J, Perkins C L, To B and Noufi R 2008 *Prog. Photovoltaics Res. Appl.* **16** 235
[50] Oikkonen L, Ganchenkova M G, Seitsonen A P and Nieminen R 2011 *J. Phys.: Condens. Matter* **23** 422202
[51] Domain C, Laribi S, Taunier S and Guillemoles J 2003 *J. Phys. Chem. Solids* **64** 1657
[52] Wen L S 1991 *The Physical Foundation of the Solid Material Interface* (1st edn.) (Beijing: Science Press) p. 128 (in Chinese)